Ferroelectric properties of BaTiO<inf>3</inf> thin films co-doped with Mn and Nb

Ferroelectric properties of $BaTiO_3$ thin films co-doped with Mn and Nb

Cite as: AIP Advances **9**, 095207 (2019); https://doi.org/10.1063/1.5118869
Submitted: 05 July 2019 • Accepted: 30 August 2019 • Published Online: 09 September 2019

Dibya Phuyal, Soham Mukherjee, Somnath Jana, et al.

Ferroelectric properties of $BaTiO_3$ thin films co-doped with Mn and Nb

Cite as: AIP Advances 9, 095207 (2019); doi: 10.1063/1.5118869
Submitted: 5 July 2019 • Accepted: 30 August 2019 •
Published Online: 9 September 2019

Dibya Phuyal,[1,a] Soham Mukherjee,[1] Somnath Jana,[1,b] Fernand Denoel,[1] M. Venkata Kamalakar,[1] Sergei M. Butorin,[1] Alexei Kalaboukhov,[2] Håkan Rensmo,[1] and Olof Karis[1]

AFFILIATIONS

[1] Division of Molecular & Condensed Matter Physics, Department of Physics & Astronomy, Uppsala University, Box 516, SE-75121 Uppsala, Sweden
[2] Department of Microtechnology and Nanoscience, Chalmers University of Technology, S-41296 Gothenburg, Sweden

[a] **Corresponding Author:** dibya.phuyal@physics.uu.se
[b] **Present Address:** Methods and Instrumentation for Synchrotron Radiation, Helmholtz-Zentrum Berlin, 12489 Berlin, DE

ABSTRACT

We report on properties of $BaTiO_3$ thin films where the bandgap is tuned via aliovalent doping of Mn and Nb ions co-doped at the Ti site. The doped films show single-phase tetragonal structure, growing epitaxially with a smooth interface to the substrate. Using piezoforce microscopy, we find that both doped and undoped films exhibit good ferroelectric response. The piezoelectric domain switching in the films was confirmed by measuring local hysteresis of the polarization at several different areas across the thin films, demonstrating a switchable ferroelectric state. The doping of the $BaTiO_3$ also reduces the bandgap of the material from 3.2 eV for $BaTiO_3$ to nearly 2.7 eV for the 7.5% doped sample, suggesting the viability of the films for effective light harvesting in the visible spectrum. The results demonstrate co-doping as an effective strategy for bandgap engineering and a guide for the realization of visible-light applications using its ferroelectric properties.

I. INTRODUCTION

$BaTiO_3$ (BTO) is one of the most well studied ferroelectric materials with a wide range of properties that has proven its significance for both fundamental understanding and its use in ferroelectric tunnel junctions,[1] diodes,[2] and a host of different applications.[3–6] Its sizable room-temperature polarization has been a core feature in designing new devices in addition to find novel phenomena in oxide heterostructures.[7–10] Recent advances in oxide epitaxy have enabled the synthesis of new ferroelectric materials as well as a precise control of atomically sharp oxide interfaces. Strikingly, the coherent strain imposed by epitaxy results in enhanced ferroelectricity at higher transition temperatures, a higher remnant polarization of 70 $\mu C/cm^2$, an increase of nearly 250% compared to bulk $BaTiO_3$ single crystals[11] (26 $\mu C/cm^2$). Such aspects in ferroelectric thin films have stimulated further interest in the realization of unconventional phases and highlighted the necessity of fabricating thin films in device applications. Much of its functional properties can be manipulated via controlled doping to tune crystal structure, bandgap, and ferroelectricity to innovate new materials for energy harvesting.[12–14]

An often explored route to finding new functionality in BTO has been through doping with different cation substitutions at the A- or B-site in the ABO_3 perovskite crystal structure.[15,16] Co-substitution in the perovskite lattice (A-site and B-site) has been attempted by various researchers to obtain a variety of functional properties.[17,18] Recent results have shown ferromagnetic behavior appearing with Fe and Mn doping,[19,20] coupling ferroelectricity with ferromagnetic order to achieve the much sought after magnetoelectric effect.[21–24] Ferroelectric BTO is also known to produce a bulk-photovoltaic effect where photovoltages larger than its bandgap have been reported,[25–27] which has triggered a resurgence of research into ferroelectric photovoltaics.[28–30] The underlying concept of this photovoltaic approach is to exploit the remnant polarization of the ferroelectric to promote the separation of photo-generated electron-hole pairs and extend light absorption into the visible range.[31–33] However, the distortion introduced by transition metal dopants with partially filled *d*-orbitals competes

directly with ferroelectricity in $BaTiO_3$[34,35] – making this strategy non-trivial.

In this direction, we recently demonstrated the effects of aliovalent doping by Mn^{3+} and Nb^{5+} at the Ti-site on the bandgap and ferroelectric properties of $BaTi_{1-x}(Mn_{1/2}Nb_{1/2})_xO_3$ (abbreviated hereafter as BTMNO) polycrystalline ceramics.[36] The impurity levels decreases the overall bandgap from about 3.2 eV for the pure BTO to 1.7 eV for the $x = 0.075$ doped polycrystalline samples in bulk form. This reduction was due to generation of Mn *d* states at the edge of the valence band.[37] The saturation polarization was found to remain at 70% of its bulk BTO counterpart value. Room-temperature ferroelectricity is lost for doping levels beyond $x > 0.075$, where the compound adopt a high symmetry cubic structure at room temperature. In this letter, we extend our previous investigations of bulk-doped BTO to the realization of new types of thin films based on Mn and Nb co-doped BTO grown by pulsed laser deposition (PLD) and investigate their epitaxial growth and crystallinity, microstructure, ferroelectricity, and changes to the bandgap. We explore Mn/Nb doping levels for $x = 0.025$, which in our previous study of bulk materials, was found to exhibit the highest saturation polarization at 22.3 $\mu C/cm^2$, and $x = 0.075$ (lowest band gap) in addition to the parent $BaTiO_3$ thin films. The ferroelectric hysteresis and domain switching observed through piezoresponse force microscopy (PFM) measurements indicates that the BTMNO thin films maintain a good ferroelectric response. The bandgap also systematically shifts towards the visible light region with increasing doping (E_g of 2.7 eV for $x = 0.075$), further demonstrating the effectiveness of co-doping at the B site with promising photovoltaic and other optoelectronic applications.

II. SAMPLE PREPARATION AND EXPERIMENTAL PROCEDURE

Thin films of BTO and $BaTi_{1-x}(Mn_{1/2}Nb_{1/2})_xO_3$ ($x = 0.025$, 0.075) were grown on TiO_2-terminated 0.5% Nb-doped $SrTiO_3$(001) substrates with a 0.1° miscut. The targets were ablated with KrF excimer laser ($\lambda = 248$ nm) at 1 J/cm^2 for the BTO samples and 1.3 J/cm^2 for the BTMNO respectively. The film was deposited at 650 °C and an oxygen pressure of 0.05 mBar. After deposition, the films were post-annealed *in-situ* at 650 °C and 1000 mBar of O_2 for 1 h prior to cooling at a rate of 5 °C/min to room temperature.

The phase purity and structural analysis were performed using a four-circle high-resolution X-ray diffractometer (PANalytical X'Pert-PRO) with Cu Kα radiation and thickness was estimated using x-ray reflectivity (XRR). The surface morphology was examined by Atomic Force Microscopy (AFM, Bruker Multimode 8) and cross-sectional scanning electron microscopy (SEM) images were done using a Zeiss Merlin with an acceleration voltage of 10 kV. Local ferroelectric polarization was studied using piezoresponse force microscopy (PFM, Bruker Dimension ICON) using conductive Co/Fe coated 10 μm Si_3N_4 tips at 20 kHz. PFM poling measurements were conducted using Pt/Ir coated tips. Piezoelectric hysteresis loops were measured at fixed locations on the film surface as a function of dc switching bias. The amplitude (R) and phase (θ) of the piezoelectric signals were measured using a lock-in amplifier. The band gap measurements were made with a Pelkin-Elmer UV-Vis measured in reflectance mode and converted to the absorbance spectra by the Kubelka-Munk method.[38] Hard x-ray photoelectron spectroscopy (HAXPES) measurements were done to probe valence electronic structure using 5.96 keV excitation energy at PETRA III beamline P09.[39] The exciting X-rays were monochromatized by a combination of a Si(111) double-crystal primary monochromator and a Si(333) channel-cut post-monochromator to attain a high energy resolution. Energy calibration was done with a clean Au foil with Fermi level set to 0 eV.

III. RESULTS AND DISCUSSION

Fig. 1 shows the x-ray 2θ-ω diffraction scans of the BTO and BTMNO films grown on 0.5% Nb-doped $SrTiO_3$ (001) substrates. The three clear diffraction peaks correspond to (00*l*) reflections. No indication of any secondary phases is observed. As shown in Fig. 1, (00*l*) XRD peaks observed from the underlying STO substrates (sharper peaks marked by open squares) and the deposited films (*filled black circles*) are well separated. The Mn/Nb-doped films exhibit all three major (00*l*) reflections indicating that the parent

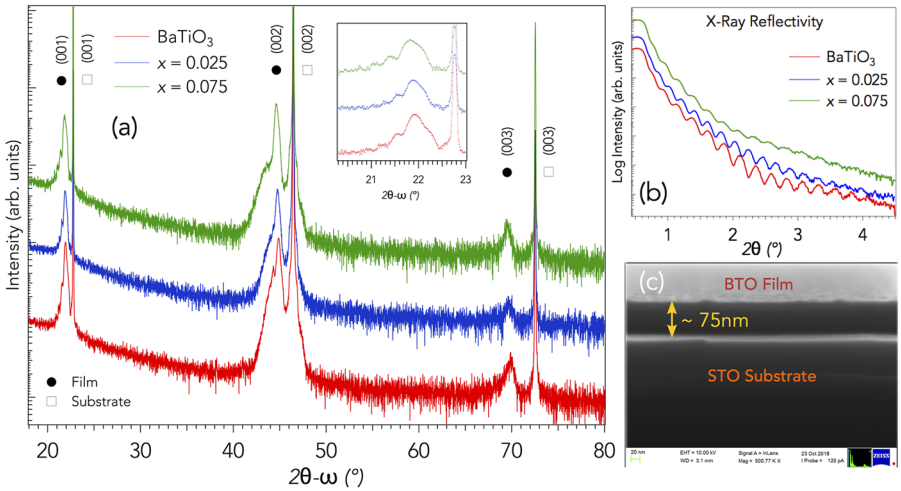

FIG. 1. (a) XRD scans of the $SrTiO_3/BaTiO_3$ and two doped films. The inset shows the reflection near the (001) peak, which show interference fringes as result of a smooth interface with the substrate. (b) X-ray reflectivity showing Keissig fringes that indicate a smooth interface. (c) Cross-sectional SEM image of the BTO thin films on 0.5% Nb doped $SrTiO_3$ substrate showing smooth interface.

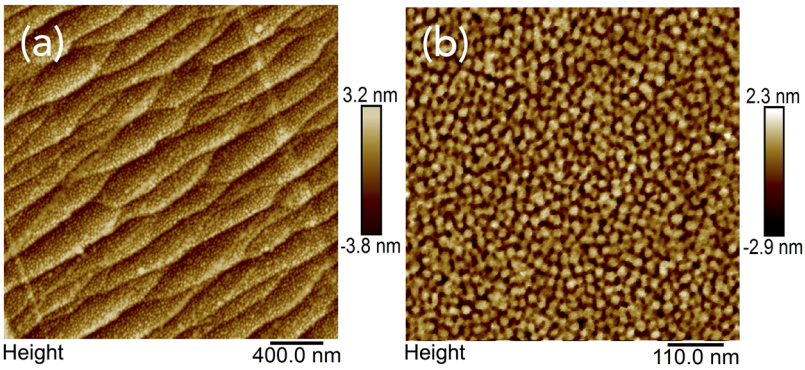

FIG. 2. AFM images of (a) 75 nm doped BTMNO-75 film with well-defined terraces indicating layer-by-layer growth. (b) 125 nm $BaTiO_3$ thin films with 3D nucleated clusters show a uniform and dense microstructure with film roughness of ~ 0.8 nm.

BTO and BTMNO films are highly oriented on the STO substrates. The position of (002) peaks systematically shifts towards lower 2θ values with increasing Mn/Nb content, suggesting an enlargement of the *c* lattice parameter as well as the two transition metals occupy the B-site. The out-of-plane (*c* axis) lattice parameters calculated from the (002) reflections are 4.036 Å, 4.049 Å, and 4.058 Å for BTO, BTMNO-25, and BTMNO-75 respectively, showing a relaxed thick film that is comparable to *c*-axis of bulk BTO (4.036 Å). The volume expansion of the unit cell is likely a result of larger ionic radii of Mn^{3+} (78.5 pm) and Nb^{5+}(78 pm) ions occupying Ti^{4+} (74.5 pm)[34] sites. The inset of Fig. 1 shows expanded region around the (001) peak, with reflections clearly displaying interference fringes suggesting a relatively coherent and a smooth interface with the $SrTiO_3$(001) substrate. This has also been confirmed from cross-sectional SEM image obtained for BTMNO thin films, a representative figure for the series is shown in Fig. 1(c).

Fig. 2 shows the film morphology from AFM images for the three samples. Since the samples are grown on an STO substrate with a 0.1° miscut, the step-terrace structure of the deposited film post-annealing is clearly observed in the AFM image shown in Fig. 2(a). This indicates atomically flat terraces with single unit-cell steps (~ 4 Å). For thicker films, 3D clusters nucleate on these layers due to the stress induced by the lattice mismatch (Fig. 2(b)).[20]

We characterize the light-absorption properties of the BTO and doped BTO films using a UV-Vis spectrometer in the total reflectance mode (F(R)) as shown in Fig. 3. The figure clearly shows redshift in the absorption for the doped materials in comparison with the parent compound. The bandgap of $BaTiO_3$ has previously been reported to be nearly 3.2 eV, just outside of the visible spectrum.[36] Here, the optical band gaps could be estimated from the tangent lines in the $(\alpha h\nu)^2$ versus $h\nu$ plots for the three samples. The BTMNO-75 shows a bandgap of approximately 2.7 eV, enabling the absorption of sunlight in the visible range, and lower than that for BTO (3.2 eV) thin film, thereby enabling greater absorption of sunlight in the visible range. This is in line with our report on polycrystalline samples, where the bandgap reduction was shown to result from Mn *d* states hybridization with O 2*p* states at the edge of the valence and conduction bands.[37] The valence electronic structure changes to the films are measured by HAXPES and shown in Fig. 3(b). The spectra reveal a growing intensity in valence states from 8 eV extending to about 2 eV in binding energy (BE). The onset of the valence band maximum (VBM), defined from the Fermi level (E_F) at 0 eV, also sees a clear shift towards lower BE as a function of doping. The shift in the VBM energy position of BTO to BTMNO-75 sample is approximately 0.5 eV, similar to that seen in bandgap changes from UV-Vis reflectance data in Fig. 3(a). We interpret this shift in the valence band edge due admixed dopant *d* states that hybridize with O 2*p* that push the VBM towards conduction band and reduces the bandgap.

PFM is a reliable technique to trace ferroelectric hysteresis characteristics at the nanoscale and to uncover direct evidence of ferroelectricity. This technique has developed into a tool capable of directly probing ferroelectricity.[40–42] Fig. 4(a,b,c) shows the local hysteretic behavior typical of polarization switching for all three

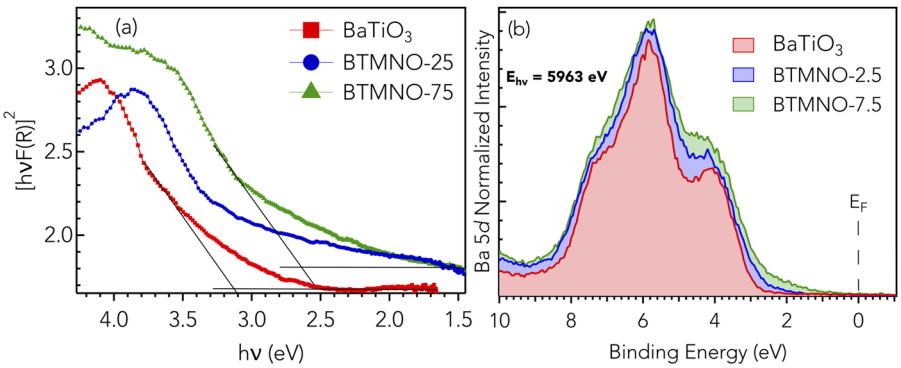

FIG. 3. (a) UV-Vis measurements in reflectance mode for BTO, BTMNO-25, and BTMNO-75 thin films with a bandgap tuning from 3.2 eV to 2.7 eV respectively. (b) Bulk valence electronic structure measured by HAXPES showing increased intensity of states and energy shift in the valence band edge towards the Fermi level (E_F).

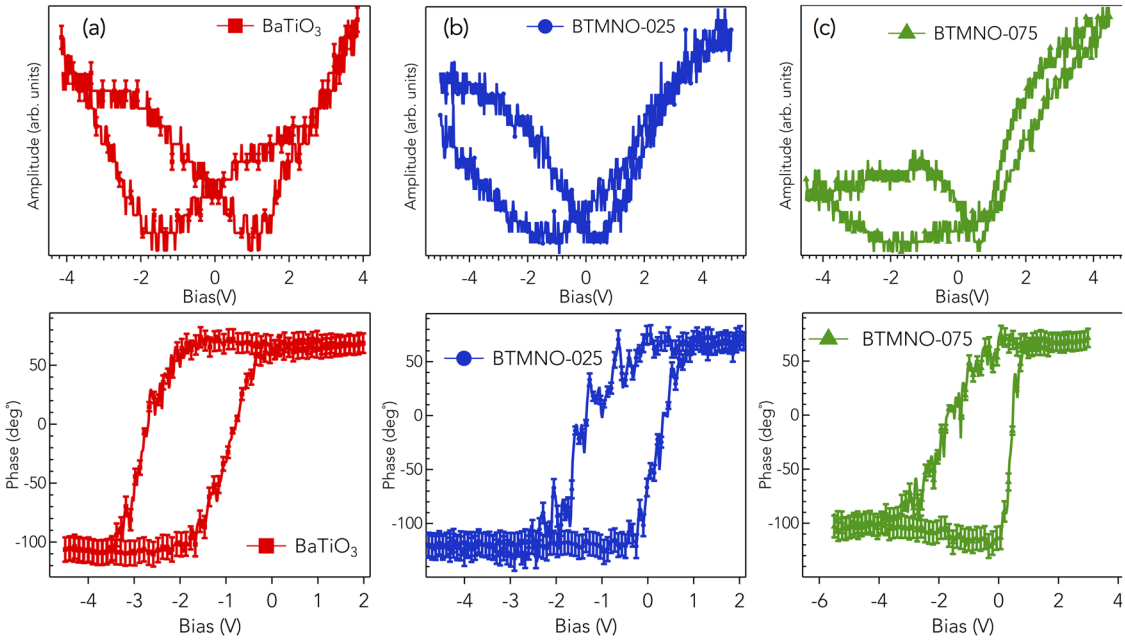

FIG. 4. PFM local amplitude (*top panel*) and hysteresis phase loops (*bottom panel*) for 75 nm films of (a) $BaTiO_3$, (b) BTMNO-25, and (c) BTMNO-75.

samples. The top panel shows the amplitude switching and bottom show the phase switching as a function of applied bias. The PFM phase-voltage curve shows a fully saturated hysteresis for the BTO and doped BTMNO samples. All curves show an 180° phase change across the saturation voltages, signifying a ferroelectric that is fully switched. The hysteresis for BTMNO-075 shows a slight anti-symmetric phase with respect to negative DC bias, which can likely be attributed to polarization pinning in the upward direction.[43–46]

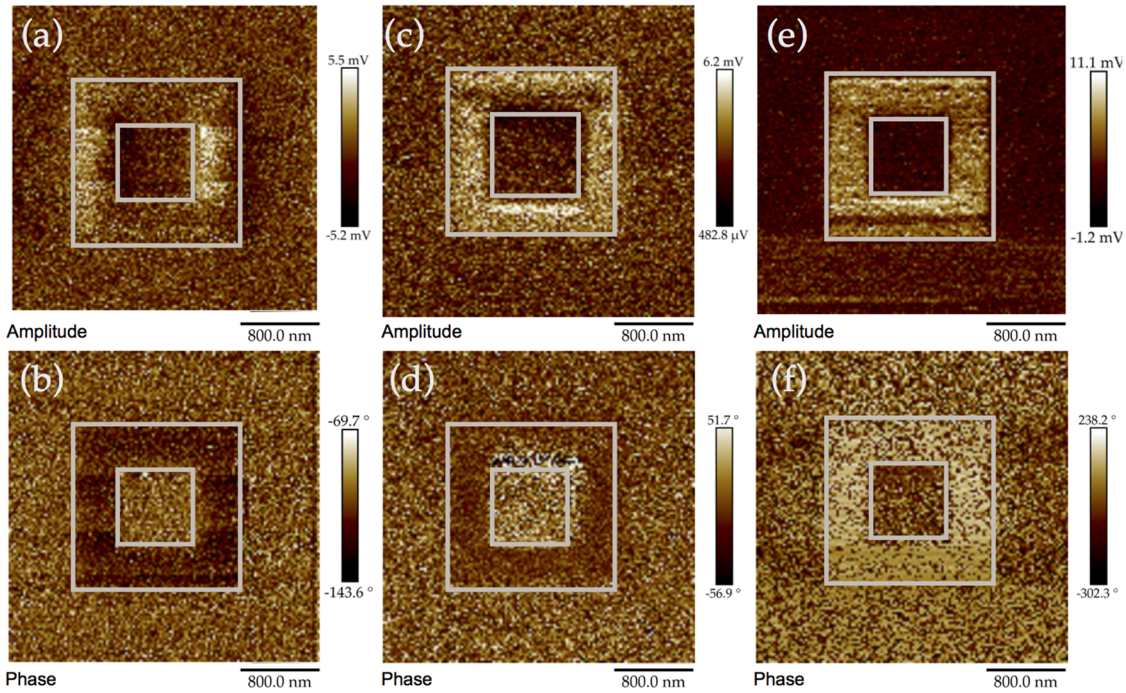

FIG. 5. PFM out-of-plane amplitude (top panel) and phase image (bottom panel) of square domains with opposite polarization directions written using an AFM tip with a bias V_{Tip} of ± 8 V for (a,b) $BaTiO_3$, (c,d) BTMNO-025, and (e,f) BTMNO-075.

Note that the hysteresis loop is offset towards a negative voltage indicating a built-in electric field that is also found in similar studies.[43] The amplitude curves (Fig. 4, *top panel*) show a nearly symmetrical butterfly shape for the $BaTiO_3$ sample, which indicates a robust and switchable ferroelectricity. The curve is slightly anti-symmetric for the BTMNO-25 and BTMNO-75 thin film samples, likely due to strong poling for the doped thin films. Both hysteresis and butterfly loops however are characteristic of classical ferroelectric switching.

To demonstrate the effect of poling on ferroelectric switching of the thin film, we reverse the upward polarization after writing alternative square patterns with +8 V and -8V biases on the PFM tip. Fig. 5 shows the resulting polarization patterns as measured by PFM through the 2 x 2 μm^2 biased area for all films. The contrast in out-of-plane (*c-axis*) PFM images is correlated with the orientation of the ferroelectric polarization, with dark (bright) region indicating upward (downward) ferroelectric polarization. The antiparallel domain line shows a clear contrast with the polarization in the opposite direction, showing a strong response to reversibility. Overall, the PFM images and the presence of hysteresis loops from ferroelectric switching strongly indicate that these films are high quality and displays good ferroelectric properties.

IV. CONCLUSION

Thin films of x = 0.025 and 0.075 $Mn_{1/2}Nb_{1/2}$ doped $BaTiO_3$ were successfully fabricated through PLD on $SrTiO_3$(001) substrates. Structural analyses showed the tetragonal films had grown epitaxially with smooth interfaces on $SrTiO_3$ substrates. UV-Vis measurements confirm that the bandgap is reduced with increasing doping content, as also evident from the valence band edge shifting towards the Fermi level observed by HAXPES. Similarly, all samples were found to exhibit ferroelectricity as confirmed from the 180° phase reversal as a function of applied bias in the piezo-force microscopy data. The local polarization of the films was also switchable across the surface, characteristic of writing on the surface after poling experiments. The combination of lower bandgap and preserved ferroelectric polarization makes these films very interesting for future exploration of light-harvesting applications innovative heterostructures.

ACKNOWLEDGMENTS

This work was supported financially in part by the Swedish Energy Agency (Grant No. P43549-1), Swedish Research Council (Grant No. 2016-4524, 2018-04330), Knut and Alice Wallenberg Foundation (2012.0031), and the Tryggers Foundation (Grant No. CTS-17:376). We also acknowledge support from the Swedish national research infrastructure for micro and nano fabrication (Myfab). We kindly thank Henrik Frederiksen for support in the fabrication of thin films.

REFERENCES

[1] M. Y. Zhuravlev, R. F. Sabirianov, S. S. Jaswal, and E. Y. Tsymbal, Phys. Rev. Lett. **94**, 246802 (2005).
[2] T. Choi, S. Lee, Y. J. Choi, V. Kiryukhin, and S. W. Cheong, Science **324**, 63 (2009).
[3] R. E. Cohen, Nature **358**, 136 (1992).
[4] M. Dawber, K. M. Rabe, and J. F. Scott, Rev. Mod. Phys. **77**, 1083 (2005).
[5] L. W. Martin and A. M. Rappe, Nat. Rev. Mater. **2**, 16087 (2016).
[6] J. F. Scott, Science **315**, 954 (2007).
[7] J. Mannhart and D. G. Schlom, Science **327**, 1607 (2010).
[8] P. Zubko, S. Gariglio, M. Gabay, P. Ghosez, and J.-M. Triscone, Annu. Rev. Condens. Matter Phys. **2**, 141 (2011).
[9] H. Y. Hwang, Y. Iwasa, M. Kawasaki, B. Keimer, N. Nagaosa, and Y. Tokura, Nat. Mater. **11**, 103 (2012).
[10] J. Tornos, F. Gallego, S. Valencia, Y. H. Liu, V. Rouco, V. Lauter, R. Abrudan, C. Luo, H. Ryll, Q. Wang, D. Hernandez-Martin, G. Orfila, M. Cabero, F. Cuellar, D. Arias, F. J. Mompean, M. Garcia-Hernandez, F. Radu, T. R. Charlton, A. Rivera-Calzada, Z. Sefrioui, S. G. E. Te Velthuis, C. Leon, and J. Santamaria, Phys. Rev. Lett. **122**, 037601 (2019).
[11] K. J. Choi, M. Biegalski, Y. L. Li, A. Sharan, J. Schubert, R. Uecker, P. Reiche, Y. B. Chen, X. Q. Pan, V. Gopalan, L.-Q. Chen, D. G. Schlom, and C. B. Eom, Science **306**, 1005 (2004).
[12] T. Shi, L. Xie, L. Gu, and J. Zhu, Sci. Rep. **5**, 8606 (2015).
[13] H. K. Chandra, K. Gupta, A. K. Nandy, and P. Mahadevan, Phys. Rev. B **87**, 214110 (2013).
[14] T. Qi, I. Grinberg, and A. M. Rappe, Phys. Rev. B **83**, 224108 (2011).
[15] W. S. Choi, M. F. Chisholm, D. J. Singh, T. Choi, G. E. Jellison, and H. N. Lee, Nat. Commun. **3**, 689 (2012).
[16] P. Lopez-Varo, L. Bertoluzzi, J. Bisquertb, M. Alexe, M. Coll, J. Huang, J. A. Jimenez-Tejada, T. Kirchartzg, R. Nechache, F. Rosei, and Y. Yuan, Phys. Rep. **653**, 1 (2016).
[17] R. K. Katiyar, Y. Sharma, P. Misra, V. S. Puli, S. Sahoo, A. Kumar, J. F. Scott, G. Morell, B. R. Weiner, and R. S. Katiyar, Appl. Phys. Lett. **105**, 172904 (2014).
[18] S. Kumari, N. Ortega, A. Kumar, J. F. Scott, and R. S. Katiyar, AIP Adv. **4**, 037101 (2014).
[19] Y. H. Lin, J. Yuan, S. Zhang, Y. Zhang, J. Liu, Y. Wang, and C. W. Nan, Appl. Phys. Lett. **95**, 033105 (2009).
[20] E. Venkata Ramana, S. M. Yang, R. Jung, M. H. Jung, B. W. Lee, and C. U. Jung, J. Appl. Phys. **113**, 187219 (2013).
[21] A. Filippetti and N. A. Hill, Phys. Rev. B - Condens. Matter Mater. Phys. **65**, 195120 (2002).
[22] F. Matsukura, Y. Tokura, and H. Ohno, Nat. Nanotechnol. **10**, 209 (2015).
[23] N. A. Spaldin, S.-W. Cheong, and R. Ramesh, Phys. Today **63**(10), 38 (2010).
[24] M. Mostovoy, Nat. Mater. **9**, 188 (2010).
[25] S. M. Young and A. M. Rappe, Phys. Rev. Lett. **109**, 116601 (2012).
[26] A. Zenkevich, Y. Matveyev, K. Maksimova, R. Gaynutdinov, A. Tolstikhina, and V. Fridkin, Phys. Rev. B **90**(R), 161409 (2014).
[27] S. Y. Yang, J. Seidel, S. J. Byrnes, P. Shafer, C.-H. Yang, M. D. Rossell, P. Yu, Y.-H. Chu, J. F. Scott, J. W. Ager, L. W. Martin, and R. Ramesh, Nat. Nanotechnol. **5**, 143 (2010).
[28] R. Nechache, C. Harnagea, S. Li, L. Cardenas, W. Huang, J. Chakrabartty, and F. Rosei, Nat. Photonics **9**, 61 (2014).
[29] J. E. Spanier, V. M. Fridkin, A. M. Rappe, A. R. Akbashev, A. Polemi, Y. Qi, Z. Gu, S. M. Young, C. J. Hawley, D. Imbrenda, G. Xiao, A. L. Bennett-Jackson, and C. L. Johnson, Nat. Photonics **10**, 611 (2016).
[30] H. Huang, Nat. Photonics **4**, 134 (2010).
[31] H. Matsuo, Y. Noguchi, and M. Miyayama, Nat. Commun. **8**, 207 (2017).
[32] Y. Yuan, Z. Xiao, B. Yang, and J. Huang, J. Mater. Chem. A **2**, 6027 (2014).
[33] K. T. Butler, J. M. Frost, and A. Walsh, Energy Environ. Sci. **8**, 838 (2015).
[34] N. A. Hill, J. Phys. Chem. B **104**, 6694 (2000).
[35] N. A. Benedek and C. J. Fennie, J. Phys. Chem. C **117**, 13339 (2013).
[36] S. Das, S. Ghara, P. Mahadevan, A. Sundaresan, J. Gopalakrishnan, and D. D. Sarma, ACS Energy Lett. **3**, 1176 (2018).
[37] D. Phuyal, S. Mukherjee, S. Das, S. Jana, K. O. Kvashnina, D. D. Sarma, H. Rensmo, S. M. Buortin, and O. Karis, Europhys. Lett. **124**, 27005 (2018).
[38] J. Tauc, R. Grigorovici, and A. Vancu, Phys. Status Solidi **15**, 627 (1966).
[39] A. Gloskovskii, G. Stryganyuk, G. H. Fecher, C. Felser, S. Thiess, H. Schulz-Ritter, W. Drube, G. Berner, M. Sing, R. Claessen, and M. Yamamoto, J. Electron Spectros. Relat. Phenomena **185**, 47 (2012).

[40] A. Gruverman and A. Kholkin, Reports Prog. Phys. **69**, 2443 (2006).
[41] B. J. Rodriguez, S. Jesse, M. Alexe, and S. V. Kalinin, Adv. Mater. **20**, 109 (2008).
[42] N. Balke, I. Bdikin, S. V. Kalinin, and A. L. Kholkin, J. Am. Ceram. Soc. **92**, 1629 (2009).
[43] A. Gruverman, D. Wu, H. Lu, Y. Wang, H. W. Jang, C. M. Folkman, M. Y. Zhuravlev, D. Felker, M. Rzchowski, C. B. Eom, and E. Y. Tsymbal, Nano Lett. **9**, 3539 (2009).
[44] Y. J. Shin, Y. Kim, S. J. Kang, H. H. Nahm, P. Murugavel, J. R. Kim, M. R. Cho, L. Wang, S. M. Yang, J. G. Yoon, J. S. Chung, M. Kim, H. Zhou, S. H. Chang, and T. W. Noh, Adv. Mater. **29**, 1602795 (2017).
[45] B. S. Li, G. R. Li, Q. R. Yin, Z. G. Zhu, A. L. Ding, and W. W. Cao, J. Phys. D. Appl. Phys. **38**, 1107 (2005).
[46] C. M. Folkman, S. H. Baek, C. T. Nelson, H. W. Jang, T. Tybell, X. Q. Pan, and C. B. Eom, Appl. Phys. Lett. **96**, 052903 (2010).